Article

JFPE

Journal of Fire Protection Engineering
21(1) 5–36

DOI: 10.1177/1042391510394242
jfe.sagepub.com

SAGE

Model scale tunnel fire tests with point extraction ventilation

Haukur Ingason
Fire Technology, SP Technical Research Institute of Sweden, Borås, Sweden

Ying Zhen Li
School of Mechanical Engineering, Southwest Jiaotong University, Chengdu, Sichuan, China

Abstract
Experimental results are presented from a series of tests in a model scale tunnel (1 : 23). This study focuses on single and two-point extraction ventilation systems to complement a previous study with the same apparatus using longitudinal ventilation only. The point extraction ventilation system in this test series was operated under different fire loads and flow conditions of either forced longitudinal ventilation or natural ventilation. Wood crib piles were used to simulate the fire source, which was designed to correspond to a 'heavy goods vehicle' fire load at full scale. The parameters varied were the number of wood cribs, the longitudinal ventilation velocity, and the arrangement of the extraction vent openings and their exhaust capacity. Measurement data were obtained for maximum heat release rates, fire growth rates, maximum excess temperatures beneath the ceiling, and heat fluxes. Fire spread between wood cribs with a separation distance corresponding to 15 m at full scale was also investigated. These data are reproduced well by empirical correlations that were established as part of the study. It is concluded that fire and smoke flows upstream and downstream of the fire source can be fully controlled if the ventilation velocities upstream and downstream are above about 2.9 and 3.8 m/s, respectively, at full scale for a single-point extraction ventilation system and greater than about 2.9 m/s on both sides at full scale for a two-point system.

Keywords
Model scale, tunnel fire, point extraction ventilation, fire spread, longitudinal ventilation

Corresponding author:
Haukur Ingason, Fire Technology, SP Technical Research Institute of Sweden, Borås, Sweden
Email: haukur.ingason@sp.se

Introduction

Urban twin-tube road tunnels often become congested with vehicles due to heavy traffic. The most common fire safety design concept today is to install jet fans in the ceiling in order to create longitudinal flows. This design concept assumes that the traffic is stopped upstream of a fire and that the tunnel ventilation ensures that upstream of the fire the tunnel will be free of smoke. Vehicles downstream of the fire are assumed to continue driving out of the tunnel. The design of such a system assumes that the fire brigade will be able to attack the fire from the smoke-free upstream side. However, in urban areas, where there are very likely queues in the tunnel this assumption fails. Consequently, people in the cars and buses trapped in traffic queues downstream of the fire source may not be able to escape from the fire and smoke quickly by driving their cars away from the seat of the fire and the fire brigade may not be able to reach the fire and vehicles downstream of the fire due to congestion, resulting in a large number of people being put in jeopardy.

One way of solving this is to install an extraction ventilation system with large vent openings located close to the seat of the fire. Since the fire may develop at any location in the tunnel, extraction vent openings at the ceiling must be provided throughout its length. This extraction ventilation system must be powerful enough to create longitudinal inflows from two directions. In some cases, jet fans in the ceiling or inflow of air at floor level may be needed to balance the longitudinal flow and obtain satisfactory flow conditions. With this type of ventilation system, people trapped in a queue will be much better protected from smoke and the fire brigade will be able to attack the fire from both sides. In the experiments discussed here, the extraction system has been tested by using different fire loads and by combining it with longitudinal ventilation.

The extraction system can be categorized as a single-point extraction system, two-point extraction system, three-point extraction system, etc., by the number of extraction vents operating during a fire. The configuration of these systems is different. However, it is clear that the concept is essentially the same for all, in that the incoming air with a sufficiently large ventilation velocity must be supplied from both sides of the extraction points. These extraction systems can be used in a tunnel with a semi-transverse ventilation system or a transverse ventilation system. In a tunnel with a transverse ventilation system, supply vents should be closed during a fire because, if the supply vents are open, the extraction system must extract a higher gas flow, decreasing its efficiency. Because, for a given distance between vents, fire and smoke flow will spread a greater distance if multiple vents are used at a given total exhaust flow rate and because it is easier to control the extraction system with fewer extraction vents, the single-point extraction system and the two-point extraction system are the focus here.

Most of the knowledge about smoke and fire spread in tunnels has generally been obtained from large-scale testing, such as Runehamar tunnel tests [1,2], the Memorial Tunnel Test Program [3], or the EUREKA 499 [4]. Large-scale testing is, however, expensive, time consuming, and logistically complicated to perform. The information obtained is often incomplete due to the limited number of tests and

lack of instrumentation. Large-scale testing is, however, necessary to obtain acceptable verification of model scale results. Model scale tests can be used to complement large-scale testing, provide information which is difficult to obtain otherwise, and allow parametric studies too expensive on a large scale.

Vauquelin et al [5,6]. carried out a series of model scale experiments with a helium/nitrogen gas mixture in an isothermal test-rig to investigate the extraction capability and efficiency of a two-point extraction system. A symmetrical two-point extraction system was used in their experiments, ignoring the probable longitudinal ventilation velocity across the fire site. It is noted in [5,6]. that when total exhaust volumetric flow rate is up to 370 m^3/s at full scale, smoke flow was just prevented from spreading across the extraction vents and completely controlled for a heat release rate of 10 MW in a tunnel with a height of 5 m and width of 10 m at full scale. For a heat release rate of 4 MW the corresponding exhaust volumetric flow rate is 279 m^3/s. They also proposed that the total exhaust volumetric flow rate can be much smaller if it is sufficient that the smoke flow is confined to an acceptable zone, downstream of the vents. The ventilation velocity induced by extraction, which is necessary to prevent the smoke layer development after the last extraction vent has been activated, was defined as the 'confinement velocity'. The total exhaust volumetric flow rate was 201 m^3/s, corresponding to a confinement velocity of 2.01 m/s, for a heat release rate of 10 MW and 161 m^3/s, corresponding to a confinement velocity of 1.61 m/s, for a heat release rate of 4 MW. The smoke flow was confined between the portal and the exhaust point when the total exhaust volumetric flow rate was 337 m^3/s (4 times the smoke flow rate of the fire source) for a heat release rate of 20 MW. By extrapolating these data, the total exhaust volumetric flow rate should exceed 485 m^3/s, to completely control the smoke flow development, for a heat release rate of 20 MW.

According to the results from Vauquelin et al., [5,6] it would seem impossible to prevent smoke flow from spreading downstream of the extraction vents, using a two-point extraction system, for a large fire, that is, a fire involving a heavy goods vehicle (HGV) or several HGVs with a heat release rate of from 100 to 300 MW. However, the cold gas entrainment method in Vauquelin et al. [5,6] results in experimental inaccuracy compared to tests with a real fire source, for which smoke mainly consists of air entrained in the process of fuel combustion and smoke spread. For example, the method of Vauquelin et al. [5,6] injects a mixture of helium and air with flow rates of 45.4 and 84.3 m^3/s into the system to simulate a fire source having heat release rates of 10 and 20 MW, respectively, at full scale. Clearly, the extra gas flow thus introduced is comparable to the total exhaust volumetric flow rate. In addition, the method of cold gas ignores the heat transfer between the hot gases and the tunnel walls, which dominates the smoke temperature decrease along the tunnel. Both these simulation errors make it more difficult for the extraction system to control or confine the smoke flow.

In this article, experimental results from a series of tests in a model scale tunnel focusing on point extraction ventilation systems are presented. Model scale tunnel fire tests performed in the same test series but focusing only on longitudinal

ventilation has been published by the authors in Ingason and Li [7]. In the present study the interval distance between two extraction vents, the geometry of extraction vents, the extraction flow rate of the extraction vents, and different ventilation systems are taken into account. The main objective of this study is to confirm whether a large tunnel fire involving a HGV fire or several HGVs, with heat release rates from 100 to 300 MW, can be controlled or confined in an acceptable zone using a point extraction ventilation system and how to establish such control, if possible, in combination with longitudinal flow. In addition, the maximum heat release rate, the fire growth rate, the maximum excess temperature below the ceiling, and the fire spread to other neighboring wood cribs are also investigated in the model scale tests with extraction ventilation.

Theoretical considerations

Scaling theory

The model used in the present study was built at a scale of 1 : 23, which means that the size of the tunnel is scaled geometrically according to this ratio. The method of scaling being used in the tests is the widely used Froude scaling. Clearly, it is impossible and not necessary to preserve all the terms obtained by scaling theory simultaneously in model scale tests. The terms that are most important and most related to the study can be preserved. The thermal inertia of the involved material, turbulence intensity, and radiation are not explicitly scaled, but the heat release rate (HRR), the test time, flow rates, the energy content, and mass are scaled, as shown in Table 1. The scenario of a tunnel fire is very different with an open fire or an enclosure fire. Firstly, the ratio of tunnel length to tunnel height should be large enough to simulate a realistic tunnel fire. It is very expensive to build a model tunnel on a large scale. Secondly, in the model tunnel fire tests, there are always ventilated flows across the fire, which makes the flows and flames more turbulent. In the authors' opinion, the scaling ratio should not be smaller than about 1 : 20 in

Table 1. A list of scaling correlations for the model tunnel.

Type of unit	Scaling	Equation number
Heat release rate (HRR) (kW)	$Q_M/Q_F = (L_M/L_F)^{5/2}$	(1)
Velocity (m/s)	$V_M/V_F = (L_M/L_F)^{1/2}$	(2)
Time (s)	$t_M/t_F = (L_M/L_F)^{1/2}$	(3)
Energy (kJ)	$E_M/E_F = (L_M/L_F)^3$	(4)
Mass (kg)	$m_M/m_F = (L_M/L_F)^3$	(5)
Temperature (K)	$T_F/T_M = 1$	(6)

L is the length scale, subscript M refers to model scale and subscript F to full scale ($L_M/L_F = 1/23$ in present case).

order to preserve the Froude Number and to avoid producing a laminar flow in the tunnel. Experience with model tunnel fire tests at this scale shows there is good agreement between model scale and full scale for many issues. Such a scaling ratio is widely used in model tunnel fire tests all over the world. Information about scaling theories can obtained from Heskestad [8,9], Quintiere [10], and Saito et al. [11].

Determination of HRR

The HRR was determined using two different measurement techniques: measuring the fuel weight loss and measuring the mass flow rate and gas concentrations in an exhaust duct connected to the tunnel. The HRR is assumed to be directly proportional to the fuel mass loss rate, $\dot{m}_f$ (kg/s), and can be calculated using the following equation:

$$Q = \dot{m}_f \chi H_T \tag{7}$$

The actual heat release rate at a measuring point in the exhaust duct downstream of the fire can be obtained using oxygen consumption calorimetry [12,13] and the following equation (without a correction due to CO production):

$$Q = 14330 \dot{m}_a \left(\frac{X_{0,O_2}\left(1 - X_{CO_2}\right) - X_{O_2}\left(1 - X_{0,CO_2}\right)}{1 - X_{O_2} - X_{CO_2}} \right) \tag{8}$$

Experimental procedure

Experimental setup

A total of 12 tests with point extraction ventilation systems were carried out. The fire load was simulated using wood cribs. Extraction ventilation was tested with different ventilation conditions – natural and forced longitudinal ventilation. The parameters tested were the longitudinal ventilation rate, the arrangement of the exhaust openings, and the exhaust capacity. Fire spread between wood cribs with a separation distance of 0.65 m, corresponding to 15 m at full scale, was also investigated.

Longitudinal ventilation was established using an electrical axial fan attached to the entrance of the model tunnel, as shown in Figure 1. The fan itself was 0.95 m long with an inner diameter of 0.35 m and 0.8 HP motor yielding a maximum capacity of 2000 m^3/h (at 1400 rpm and 7.5 mm H_2O). The rotation speed, and thereby the capacity, could be controlled by an electrical device coupled to the motor. Between the fan and the tunnel entrance a 0.8 m long rectangular plywood box with the dimensions 0.4 m wide and 0.3 m high, was mounted to create a uniform flow at the entrance of the tunnel. The rotating flow created by the axial

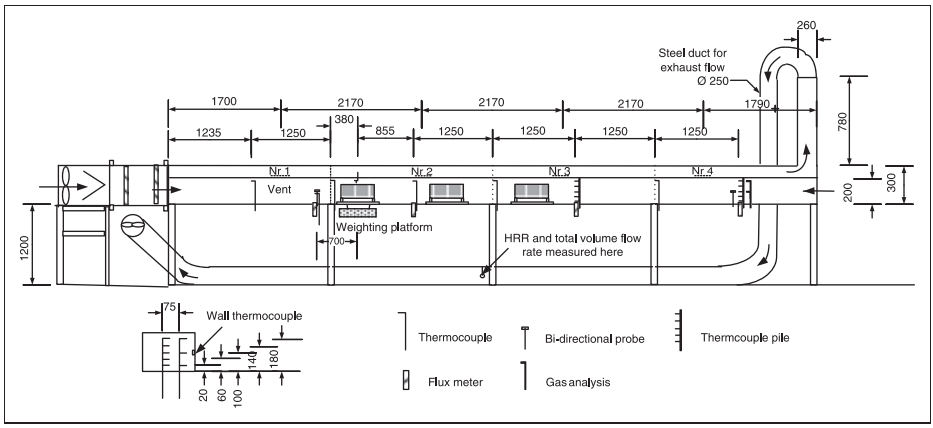

Figure 1. A schematic of the model-scale test-rig with extraction system.

fan was damped by filling the plywood box with straw fibers. Longitudinal wind velocities of 0 and 0.6 m/s were used in the test series. According to Equation (3), the corresponding large-scale velocity is 0 and 3 m/s, respectively.

The tunnel itself was 10 m long, 0.4 m wide, and 0.2 m high, as shown in Figure 1. The corresponding large-scale dimensions were 230 m long, 9.2 m wide, and 4.6 m high. The extraction ventilation channel, with a height of 0.1 m and the same width as the tunnel, was above the ceiling. The total flow rate through the extraction vents used were 0.06, 0.10, and 0.15 m^3/s, which according to Equation (2) corresponds to about 150, 250, and 380 m^3/s, respectively, at full scale. The number of exhaust openings that were used in the tests was varied between 1 and 2. In other words, in these tests a single-point extraction system and a two-point extraction system were studied. The areas of the openings were 0.026 and 0.052 m^2, respectively, which correspond to 13.75 and 27.5 m^2 at full scale.

The model was constructed using noncombustible, 15 mm thick, boards (Promatect H). The density of the boards was 870 kg/m^3, the heat capacity was 1.13 kJ/(kg·K), and thermal conductivity was 0.19 W/(m·K). The floor, ceiling and one of the vertical walls were built in Promatect H boards while the front side of the tunnel was covered with a fire resistant window glazing. The 5 mm thick window glazing (0.6 m wide and 0.35 m high) was mounted in a steel frame which was measured 0.67 m × 0.42 m (Figures 1 and 2).

The fire load consisted of a wood crib (pine). In the earlier tunnel fire tests with only longitudinal ventilation [7], two different types of wood cribs, A and B were used. Only wood crib B, a detailed description of which is given in Figure 3, was used in this study. More detailed information about the wood cribs for each test is given in Table 2. The total weight of the wood cribs used ranged from 0.91 to 1.24 kg and the total fuel surface area of wood crib B was estimated to be 0.56 m^2.

Various measurements were made during each test. The first wood crib was placed on a weighing platform (W), consisting of a scale attached by four steel rods to a free floating dried Promatect H board measuring 0.65 m long, 0.35 m

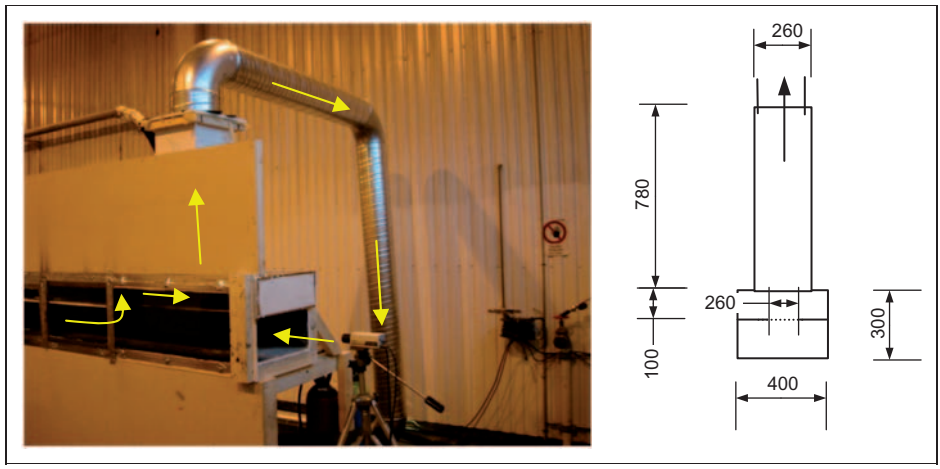

Figure 2. A schematic drawing of the model tunnel used for extraction ventilation.

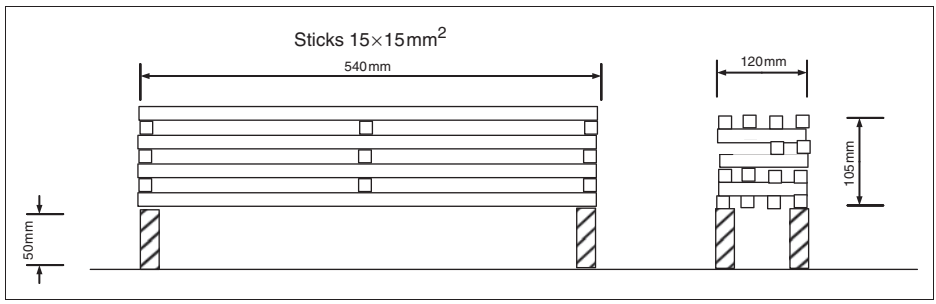

Figure 3. Detailed drawing of the wood crib used.

wide, and 0.12 m thick. In the case when more than one wood crib was used in the tests, only the first wood crib was weighed and the total heat release rate was measured using oxygen consumption calorimetry in the exhaust duct. The weighing platform was connected to a data logging system recording the weight loss every second. The center of the weighing platform was 2.87 m from the tunnel entrance ($x = 0$) and the accuracy of the weighing platform was $\pm$ 0.1 g.

Temperatures were measured with welded 0.25 mm type K thermocouples (TC). The locations of the thermocouples are shown in Figure 1, and the channel numbers and the identification of the instruments used are presented in Figure 4. Most of the thermocouples were placed 0.02 m below the ceiling along the tunnel centerline. A pile (or rake) of thermocouples was placed 6.22 m (pile A in Figure 4) and 8.72 m (pile B in Figure 4) from the inlet opening, respectively. The thermocouples of pile A and B were placed at the centerline of the tunnel and 0.02, 0.06, 0.10, 0.14, and 0.18 m above the floor. Additional thermocouples were placed at a distance of 0.075 m from the tunnel wall at pile B and at heights of 0.02, 0.10, and 0.18 m above

Table 2. Summary of tests carried out with extraction ventilation.

Test no.	T_a (°C)	Initial average longitudinal velocity (m/s)	Number of wood cribs	Wood crib #-weight (kg)	Open vent locations	Area of open vents (m^2)	Total volumetric flow rate in the vents, $\dot{V}_{ex}$ (m^3/s)
1	20.6	0.60	1	1.048	Nr 4	0.052	0.15
2	19.8	0	1	1.060	Nr 2	0.026	0.14
3	21.0	0	1	1.002	Nr 1	0.026	0.09
4	21.5	0	2	1.114	Nr 2	0.052	0.14
5	22.2	0	1	1.046	Nr 1	0.026	0.06
6	21.2	0.60	1	1.138	Nr 2	0.026	0.14
7	21.7	0.60	2	#1-1.128 #2-1.142	Nr 4	0.052	0.14
8	20.7	0.60	3	#1-1.158 #2-1.052 #3-1.236	Nr 4	0.052	0.14
9	21.1	0	1	1.106	Nr 1, Nr 2	0.026	0.09
10	20.9	0	1	0.960	Nr 1, Nr 2	0.026	0.14
11	20.1	0	2	0.906	Nr 1, Nr 2	0.052	0.09
12	22.0	0	1	1.028	Nr 2, Nr3, Nr 4	0.026	0.14

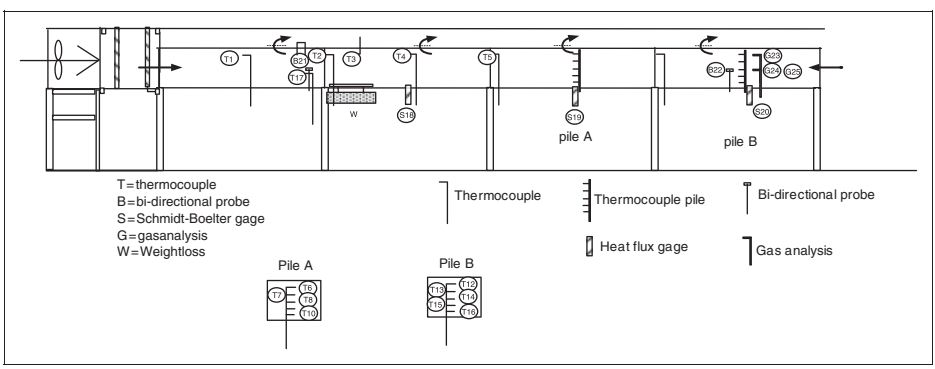

Figure 4. The channel number and identification of all the instruments.

floor level. A thermocouple was also attached to the side wall 0.10 m above the floor and 8.72 m from the tunnel entrance.

A bi-directional [14] probe (BD) was placed at the centerline of the tunnel 8.72 m from the inlet (at pile B). Another bi-directional probe was placed upstream of the fire at the center of the cross-section and 1.15 m from the inlet. The pressure

difference was measured with a pressure transducer with a measuring range of ±20 Pa. A hot-wire anemometer was also used to measure the velocities at the portals of the model tunnel.

At three locations and flush to the floor board, water-cooled heat flux gages of the Schmidt-Boelter type were placed to record the total heat flux. The locations were 3.72 m (Flux 1), 2.165 m (Flux 2), and 8.72 m (Flux 3) from the tunnel entrance ($x = 0$) in most tests. However, in tests 7 and 8, the gage at 2.165 m (Flux 2) was moved downstream of the fire to a location at 6.22 m.

Gas concentrations (O_2, CO_2, and CO) were measured 8.72 m from the entrance (at pile B) using two measuring probes consisting of short lengths of open copper tubes (Ø 6 mm). These were located at two different heights, 0.10 m and 0.175 m above the floor. Oxygen concentration was measured with an M&C Type PMA 10 (0–21%), while CO_2 (0–10%) and CO (0–3%) were measured with a Siemens Ultramat 22.

A bi-directional probe, an oxygen probe, and a thermocouple were mounted in the center of the 0.25 m diameter steel exhaust duct on the floor, at the location shown in Figure 1. Since the exhaust duct flow at the measuring point is expected to be fully developed, a flow rate can calculated from the centerline measurements.

The weighing platform, the thermocouples, the pressure transducers, the gas analyzers, and heat flux gages were all recorded at a rate of about 1 scan/s.

Test procedure

The wood cribs used in each test were dried overnight in a furnace at 60°C (<5% moisture). The first wood crib was placed on the weighing platform at a height 50 mm above the floor. A cube of fiberboard (measuring 0.03 m × 0.03 m × 0.024 m) was soaked in heptane (9 mL) and placed on the weighing platform board at the upstream edge of the wood crib. At 2 min after starting of the data logging system, this cube was ignited.

In Table 2, detailed information on each test carried out is presented. A total of 12 tests were carried out, including 8 tests with the single-point extraction system (Test 1–Test 8), 3 tests with the two-point extraction system (Test 9–Test 11), and 1 test with a three-point extraction system (Test 12).

These tests were carried out with the same tunnel width and ceiling height, 0.4 and 0.2 m, respectively, and type of wood crib but varying the number of burning wood cribs and the number of extraction vent openings in the ceiling. In tests with more than one wood crib, the separation distance between the cribs was 0.65 m. This means that the center to center distance between the cribs was 1.19 m. An extra Promatect H board was placed under wood crib No. 2 and wood crib No. 3 in order to maintain the same distance between the top of the wood crib and the ceiling.

The center-to-center distance of the ceiling openings (vents) always equaled 2.17 m, which corresponds to 50 m at full scale. The distance from the tunnel entrance to the center of the opening Nr 1 was 1.7 m (Figure 1). The area of the openings was either 0.026 m^2 or 0.052 m^2. The width of the openings was kept the

same during all tests, 0.026 m, while the length (in the x-direction) was either 0.1 or 0.2 m. The size of the openings corresponds to 13.75 and 27.5 m^2 at full scale, respectively. The steel duct was connected to the central ventilation system used to ventilate the fire test hall. The flow rate was determined before each test by regulating a valve between the steel duct and the central ventilation system. The total exhaust airflow in the steel duct was 0.06, 0.10, and 0.15 m^3/s, corresponding to about 150, 250, and 380 m^3/s, respectively, at full scale.

Test results

Detailed results for each test are given in Ingason and Li [15]. A summary of these results is presented here.

Flow conditions and heat release rate

In Table 3, the main test results related to the air flow conditions and the HRRs are given. The test number is given in the first column. The second column and third column contain the average air velocities, V_{left} and V_{right}, measured near the left portal and right portal, respectively. The fourth column shows the measured total mass flow rate in the extraction vents. The fifth column shows the fuel mass burning rate at the maximum heat release rate, $\dot{m}_{f,\max}$. The sixth column shows the maximum heat release rate based on Equation (7) for single wood crib or Equation (8) for several wood cribs. A combustion efficiency of $\chi = 0.9$ was applied in Equation (7). This value was multiplied by the heat of combustion of 16.7 MJ/kg obtained from the free burn test. The calculated heat release rates using Equation (7) and (8) show good agreement. The parameter $t_{\max}$ is the time in (min) from ignition when the maximum heat release rate occurs. The fire growth rate, $\Delta Q/\Delta t$, is taken from the time when the heat release rate is 20 kW up to the time when it reaches 50 kW. During this period the fire growth rate was comparatively linear in most cases. The ninth column contains $q''_{\max}$ the maximum heat release rate per exposed fuel surface area, that is, $q''_{\max} = Q_{\max}/A_s$.

Gas temperature

Test results related to the measured gas temperatures are shown in Table 3. The maximum ceiling temperature at distance X_f from the centerline of the fire source is shown in columns 10 to 17. The values listed here are the maximum values measured by the thermocouple during one test. The identification and location of these thermocouples can be found in Figure 4.

Total heat flux

The total heat fluxes were registered by Schmidt-Boelter gages at floor level and different locations from the fire (identified as S18, S19, and S20 in Figure 4.). In the

Table 3. Test results related to heat release rate, gas temperature, and heat flux.

Test no.	V_{left} (m/s)	V_{right} (m/s)	$\dot{m}_{ex}$ (kg/s)	$\dot{m}_{f,max}$ (kg/s)	Q_{max} (kW)	t_{max} (mi)	$\frac{\Delta Q}{\Delta t}$ (kW/mi)	q''_{max} (kW/m)	$T_{1,max}$ −1.63[e] (°C)	$T_{2,max}$ −0.38[e] (°C)	$T_{3,max}$ 0 m[e] (°C)	$T_{4,max}$ 0.86[e] (°C)	$T_{5,max}$ 2.1[e] (°C)	$T_{6,max}$ 3.36[e] (°C)	$T_{11,max}$ 4.6[e] (°C)	$T_{12,max}$ 5.86[e] (°C)	Max flux 1 0.86[e] (kW/m^2)	Max flux 2 −0.7[e] (kW/m^2)
1[a]	0.61	1.0	0.16	0.0065	97.7	2.0	89.7	174.5	22.0	54.9	1056.9	672.8	443.6	307.2	246.9	21.0	NA	1.7
2	0.25	1.27	0.15	0.0043	65.1	3.1	27.5	116.3	178.6	762.3	860.2	656.5	21.2	21.5	21.5	21.0	14.7	5.4
3	0.73	0.26	0.15	0.0035	52.6	4.7	16.9	93.9	22.3	785.0	768.3	525.8	185.2	28.2	23.3	22.6	9.9	12.2
4	0.32	1.18	0.15	0.0057	86.6	2.6	42.9	77.3	174.2	676.4	1009.3	637.4	40.5	27.5	27.5	28.6	27.3	5.8
5	0.25	0.34	0.06	0.0038	57.6	3.3	23.3	102.9	134.5	845.5	939.3	582.3	66.0	23.2	22.8	22.6	14.3	13.9
6[a]	0.59	0.9	0.16	0.0056	83.9	2.7	50.0	149.8	24.0	60.5	1037.0	730.2	76.5	24.3	23.5	23.5	32.4	0.9
7[a]	0.57	1.05	0.17	0.0067	158.3	3.9	54.5	141.4	23.2	64.2	1004.5	807.8	865.5	543.0	409.7	26.2	46.0	16.5[d]
8[a]	0.58	0.94	0.15	0.0075	190.6	4.9	63.7	113.5	23.7	63.5	981.7	701.9	838.0	825.0	605.5	33.1	47.7	47.6[d]
9[b]	0.40	0.79	0.11	0.0034	51.4	3.7	22.2	91.8	95.6	848.6	1033.1	617.9	21.9	21.6	21.0	21.0	11.7	10.1
10[b]	0.52	0.99	0.16	0.0035	52.6	3.1	22.2	93.9	20.6	819.2	813.5	606.6	22.7	22.4	22.2	21.6	12.4	9.3
11[b]	0.36	0.81	0.10	0.0038	57.6	2.8	32.6	102.9	74.9	744.5	808.8	577.4	21.4	21.3	21.2	21.2	10.2	9.1
12[c]	0.38	1.3	0.16	0.0050	75.2	2.8	50.8	134.3	119.2	713.3	909.0	617.0	278.3	58.6	63.9	22.0	21.3	3.9

[a]Forced longitudinal ventilation; [b]Two-point extraction system; [c]Three-point extraction system; [d]Measured 3.36 m downstream of the fire source; [e]Value of X_f (m).

last two columns of Table 3, the heat fluxes measured with heat flux gages, that is, Max flux 1 and Max flux 2, are shown. Very low values of heat flux were measured by heat flux gage 3, so these are not shown. Note that the values given in Table 3 are the maximum total heat fluxes measured, which correspond well to the peak heat release rates. As the flux meters are cooled by water, they measure the total heat flux towards a surface which is colder than the surrounding walls (and glass).

Flame spread

Table 4 gives detailed information concerning flame spread between wood cribs in six of the tests. Results from two former tests carried out by Ingason and Li [7] are also listed here. Fire spread occurs in all the tests, with the exception of Test 11. The 'ignition temperature' refers to the characteristic temperature below the ceiling and above the wood crib when the wood crib is ignited, that is, TC4 for #1 and TC5 for #2.

Discussion of results

The main focus of these tests is whether the point extraction system can control or confine the fire and smoke flow to an acceptable zone. In addition, many characteristic fire dynamics parameters, for example, the maximum heat release rate and fire growth rate, maximum temperature below the ceiling, heat flux, and fire spread were investigated. Note that in the analysis of these parameters, the data from Tests No. 9, 10, and 11 with two extraction vents opened are not used. The reason for the exclusion of these tests is that the flow pattern is significantly different and the longitudinal flow and flow across the fire site are unknown. Further, in Tests 3 and

Table 4. Summary of tests for flame spread.

Test no.	Arrangement of wood cribs	Flame spread	Ignition time (Ignited object) (min: s)	Ignition temperature below ceiling (°C)	Incident heat flux[b] (kW/m^2)
4	#1, #2	Yes	3:02 (#2)	584.2	14.9
7	#1, #2	Yes	1:47 (#2)	525.7	8.8
8	#1, #2, #3	Yes	1:49 (#2)	614.5	11.2
			2:47 (#3)	583.2	–
11	#1, #2	No	–	577.4	10.5
3[a]	#1, #2	Yes	1:44 (#2)	630.2	12.0
4[a]	#1, #2, #3	Yes	1:50 (#2)	613.6	10.5
			2:29 (#3)	648.3	–

[a]Results from two former tests carried out by Ingason and Li.[7]
[b]Measured by heat flux gage 1.

5, V_{right} was used instead of V_{left} as the longitudinal ventilation velocity across the fire source (V) since only vent Nr1 was open.

Heat release rate

The wood crib configuration, tunnel ventilation, and tunnel geometry can all affect fire heat release rate. According to the experimental study of wood crib fires in Croce and Xin [16], heat release rate increases with increasing porosity and only becomes a weak function of porosity when porosity is greater than 0.7 mm. The porosity of a wood crib, P, is defined as:

$$P = \frac{A_v}{A_s} s^{1/2} b^{1/2} \tag{9}$$

where A_v is the total cross-sectional area of the vertical crib shafts, A_s is the exposed surface area of the wood crib, s is the surface-to-surface spacing between adjacent sticks in a layer, and b is the stick thickness (assuming stick width equals height).

In these model scale tests, the porosity of the wood crib was chosen as 1.24 mm so that the effect of the porosity on the heat release rate can be ignored. This means that the wood crib should not show any under-ventilation tendency during the tests.

The effect of the tunnel geometry and type of fire source was not investigated systematically here. Only one cross-section was used in these experiments and two cross-sections were used in the former tests carried out by Ingason and Li [7]. An analysis of the relationship between the heat release rate and ventilation velocity is focused on here.

Figure 5 shows the fuel mass loss rate per unit fuel surface area against the ventilation velocity across the fire source. According to the principles of oxygen consumption, the stoichiometric fuel mass loss rate per unit fuel surface area, which is also given in Figure 5, can be expressed as:

$$\frac{\dot{m}_{f,stoi}}{A_s} = \frac{Q}{\chi \Delta H_c A_s} = 0.24 \frac{A}{A_s} V \tag{10}$$

that is, it can be expressed as a function of AV/A_s. The reason why only one stoichiometric line is plotted here is that the ratio of the tunnel cross-sectional area to the fuel surface area for both wood crib A [7] and wood crib B tests are almost the same, that is, the relative error is 6.7%. However, it should still be kept it in mind that the tunnel area and the fuel surface area do have an effect on the ventilation controlled wood crib fire.

From Figure 5, it is shown that for a longitudinal ventilation velocity less than 0.35 m/s, the fuel mass loss rate per unit fuel surface area increases with the ventilation velocity, and follows the stoichiometric line. This indicates that the fire under these conditions is ventilation controlled. However, when the ventilation

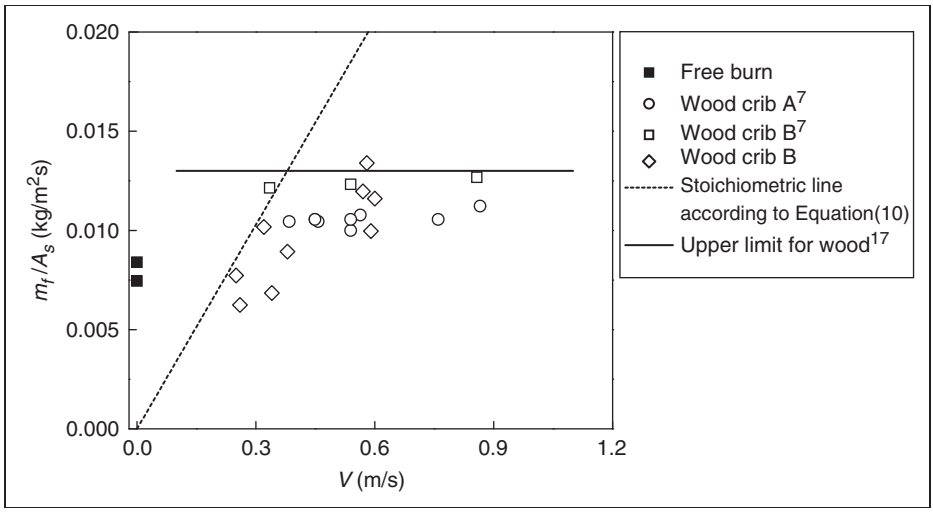

Figure 5. The maximum fuel mass loss rate per unit fuel surface area as a function of the ventilation velocity (first wood crib).

velocity rises to 0.35 m/s or more, the fire is not sensitive to the ventilation velocity. This indicates that the fire becomes fuel controlled. The upper limit of the fuel mass loss rate per unit fuel surface area is about 0.013 kg/(m^{2}s). In Tewarson and Pion [17], it was found that the maximum burning rate per fuel surface area that could be achieved with wood (Douglas fir) is 0.013 kg/(m^{2}s), which agrees well with these experimental data. The value found in Tewarson and Pion [17] is an ideal value based on the assumption that all heat losses were reduced to zero or exactly compensated by an imposed heat flux equal to the total heat loss from the fire source. Comparing the data for wood crib A and B in the fuel-controlled region, it shows that the upper limit of the burning rate per fuel area for wood crib B is slightly higher than that for wood crib A. The reason for this increase may be that the wood crib B is more susceptible to heat feedback due to the relatively lower tunnel ceiling.

It is also shown in Figure 5 that in the range of 0.35–0.9 m/s, the fuel mass loss rate per unit fuel surface area tends to be a constant, although it can be expected to decrease when the ventilation velocity is greater than a certain value due to the cooling effect of ventilation. A comparison of data shows that the ratio of fuel mass loss rate per unit fuel surface area in a tunnel fire to that in a free burn is about 1.5 in the constant (fuel-controlled) region but it can be less than 1 if the tunnel is not well ventilated.

For the two free burn tests (no wind) shown in Figure 5, it should be kept in mind that the ignition source was moved to the center of the wood cribs whereas it was located upstream of the wood crib in the model tunnel tests. The original idea of doing this was to force the wood crib to be fully involved in flames, which is similar to the case for wood cribs burning in the model tunnels. After igniting one

corner of the wood crib in a model tunnel, the ventilation and the heat feedback from tunnel walls forced the wood crib to be fully involved very quickly. As can be seen in Figure 5, the increase of the ventilation and the proximity of the walls clearly increase the maximum heat release rate for the wood cribs tested.

Figure 6 shows the maximum heat release rate per unit fuel surface area as a function of the ventilation velocity, as well as the stoichiometric value. For a fire with several wood cribs, the total fuel surface area of these wood cribs was used. According to the principles of oxygen consumption, the stoichiometric heat release rate per unit fuel surface area can be expressed as:

$$q''_{stoi} = \frac{Q}{A_s} = 3600 \frac{A}{A_s} V \tag{11}$$

From Figure 6, it is seen that the same trend as Figure 5 is present, although the data do not correlate well. The reason is that in a test with several wood cribs, all surfaces of these wood cribs are not burning at the same time. When the maximum heat release rate occurs, part of the first wood crib has started to decay. As a consequence, the maximum heat release rate divided by the total fuel surface area is slightly lower for the case with several wood cribs compared to that with a single crib.

The fire growth rate for the wood cribs against the average ventilation velocity is given in Figure 7. The fire growth rate is calculated based on data in the heat release rate range from 20 to 50 kW in these experiments. Clearly, it shows that the fire growth rate almost linearly increases with the ventilation velocity. The fire growth rate is about 3 times larger than that in a free burn test when the ventilation

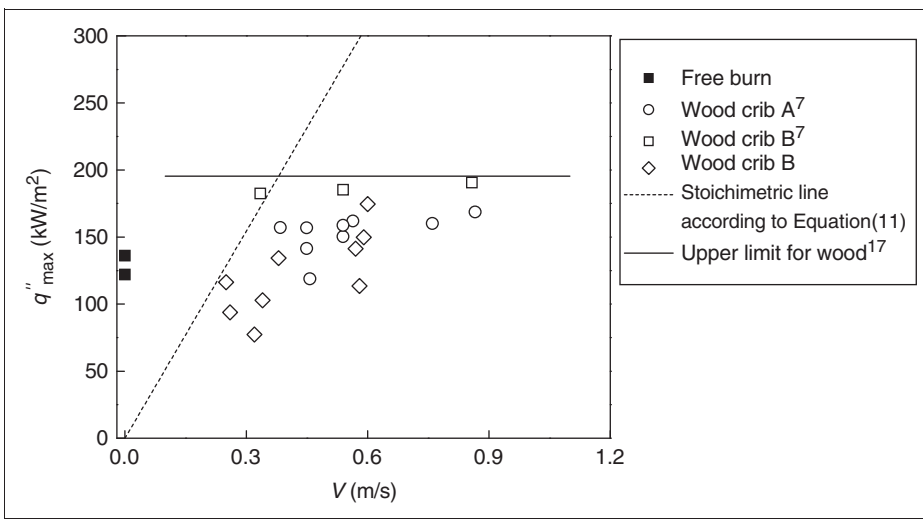

Figure 6. The maximum heat release rate per unit fuel surface area vs ventilation velocity.

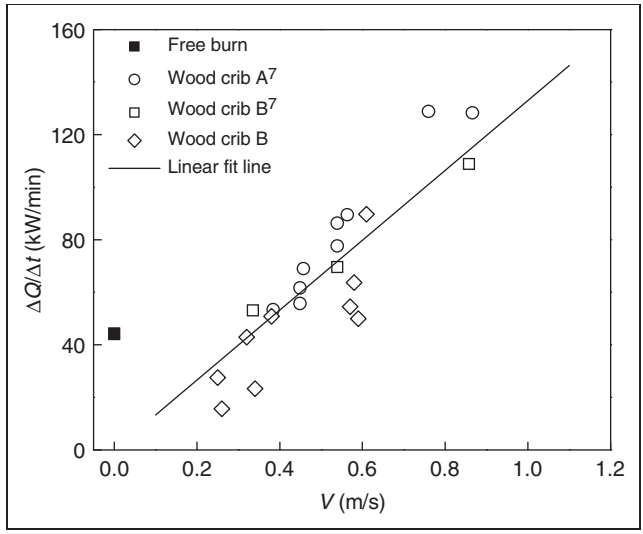

Figure 7. The fire growth rate for the wood cribs vs ventilation velocity across the fire source.

velocity equals 1 m/s (4.8 m/s at full scale). This means that the ventilation velocity plays a very important role in fire development.

From Figure 7, it is also clearly shown that the fire growth rate for a ventilation velocity of 0.3 m/s equals that in a free burn test; however, it is obviously lower for ventilation velocities below 0.3 m/s. There can be two possible explanations for this behavior. One reason is that the fire entrains more air in a free burn test than that in a tunnel fire if the longitudinal flow is very low and the fire is completely ventilation controlled. The other is that the center location of the ignition source in a free burn test makes fire development more rapid.

Maximum excess gas temperature below the ceiling

Figure 8 shows the dimensionless maximum excess temperature below the ceiling in model scale tests with point extraction ventilation combined with longitudinal and natural ventilation. The dimensionless maximum excess temperature lies mainly in a range of 3.1–3.75, corresponding to a maximum excess temperature of 900–1100°C. It seems that the maximum gas temperature beneath the tunnel ceiling is a weak function of the heat release rate and the ventilation velocity for large fires with heat release rates more than 100 MW at full scale.

According to the data on ceiling temperature in Table 3, it can be concluded that in all the tests the continuous flame zone extended to the ceiling at the maximum heat release rate. Consequently, the temperature below the ceiling in these cases represents the continuous flame zone temperature. Based on McCaffrey's fire plume theory [18], the maximum excess temperature in the continuous flame

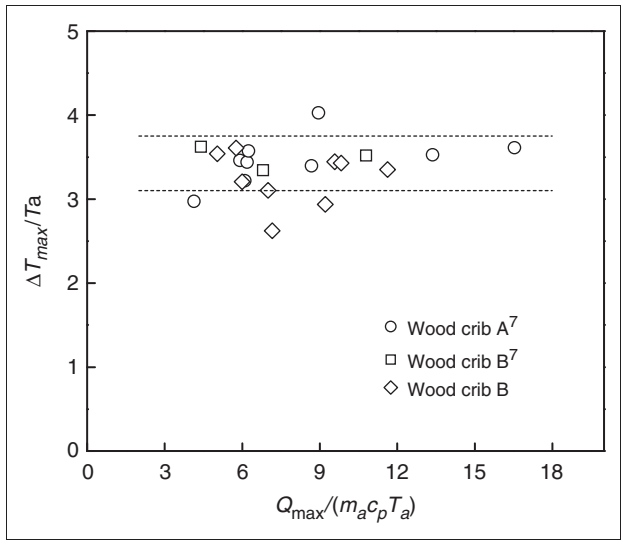

Figure 8. The dimensionless maximum excess temperature below the ceiling as a function of the dimensionless heat flow parameter.

zone is nearly constant, being mainly in a range of 700–900°C with an average value of 800°C. Consequently, one would expect that for a large fire in a tunnel, the maximum excess temperature beneath the tunnel ceiling should also be a constant if the continuous flame extends to the ceiling height, regardless of heat release rate and ventilation velocity.

However, the experimental maximum excess temperatures beneath the tunnel ceiling here are slightly higher than the 800°C proposed in McCaffrey [18]. In previous model scale tunnel fire experiments [19], the maximum excess temperature below the tunnel ceiling was also found to be 800°C. However, gas temperatures over 1000°C were measured below a tunnel ceiling in many large-scale tests [2–4]. The reason for the difference could be the presence of soot that hinders radiation loss and absorbs heat.

Total heat flux

A simple method to predict the total heat flux at the floor level is proposed here. Due to the small effect of convection on total heat flux at floor level, convection is neglected. Then the heat flux at floor level can be expressed as:

$$q''_{flux} = F\varepsilon\sigma\left(T_{cf}^4 - T_a^4\right) \tag{12}$$

The view factor F in Equation (12) is assumed to be equal to one. The emissivity, ε, was determined based on the experimental data, as shown in Figure 9.

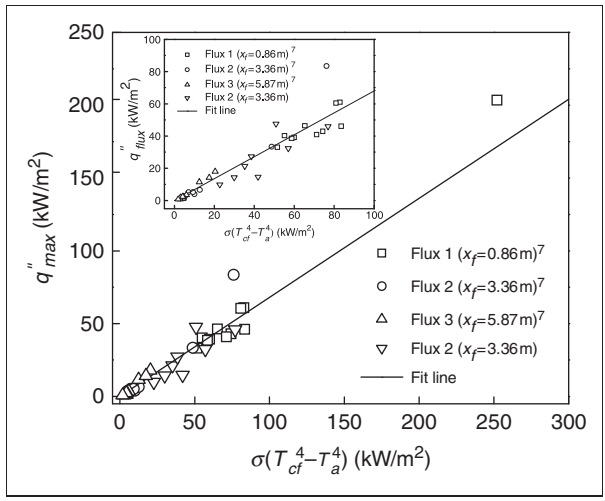

Figure 9. Determination of the emissivity defined in Equation (12).

The emissivity, ε, equals the slope of the fit line, which is determined as 0.68. There may be two reasons for this low emissivity. Firstly, the measured ceiling temperature, which can be considered as the maximum ceiling temperature above the flux gage, is higher than the average smoke temperature. Secondly, the floor temperature is a little higher than the ambient temperature. Equation (12) can be transformed into:

$$q''_{flux} = 0.68\sigma\left(T_{cf}^4 - T_a^4\right) \tag{13}$$

A linear regression coefficient of 0.950 was obtained for Equation (13). In the model scale test with longitudinal ventilation [7], there is one data point with a heat flux of 203.5 kW/m^2 (Figure 9). This data point was ignored as it would create a large error in the curve fitting of the main data. According to Equation (13), a heat flux of 171.4 kW/m^2 is predicted for this test. Equation (13) can be used to estimate the total heat flux at floor level in a tunnel fire if the temperature beneath the tunnel ceiling is known as well as the ambient temperature. It should be pointed out that all the data for the total heat flux represent peak values measured during the tests. The time of peak total heat flux correlates well with that of peak heat release rate. This implies the heat flux gage responds rapidly.

Fire spread

The second wood crib ignites when the heat flux to the wood surface reaches a certain critical value. Figure 10 shows the gas temperature beneath the ceiling when the second wood crib ignites. It is shown that the wood crib ignites when the gas

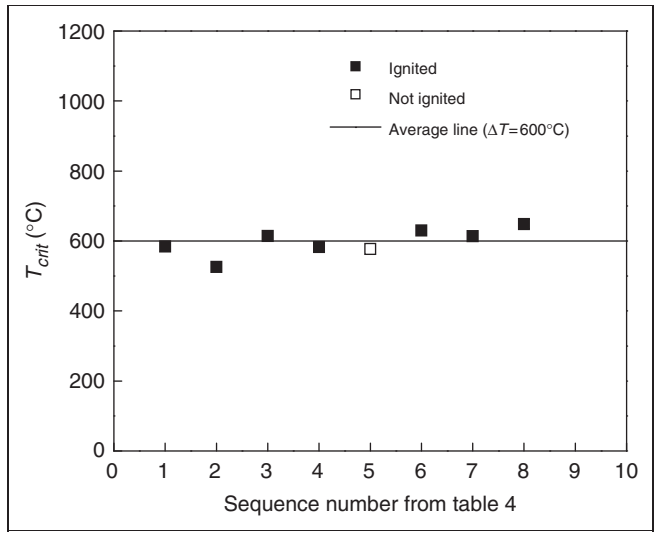

Figure 10. Critical gas temperature beneath ceiling when second wood crib ignites vs sequence of data values in 5th column of Table 4.

temperature beneath the ceiling and above the wood crib is in a range of 520–650°C. An average value of 600°C was found for the critical gas temperature beneath the ceiling for all the tests involving fire spread. Based on this information, it is easy to determine whether the wood crib may ignite or not. According to Equation (13), a critical heat flux of 22.1 kW/m^2 is found for the wood crib assuming the ambient temperature of 20°C.

Data from Test 11 without ignition was also given for comparison in Figure 10. Note that in Test 11, although the gas temperature above the wood crib rose up to 577°C, the wood crib did not ignite. However, it was observed in this test that one corner of the wood crib towards the extraction vent was charred, and the wood crib should be in a critical condition.

It is also observed that, in the tests involving fire spread, the wood crib ignited soon after the flame crawled above this wood crib. This indicates there is a close relationship between the flame length and fire spread. According to the above analysis, a critical gas temperature of about 600°C above the wood crib is required for its ignition. It is also known that the temperature of the flame tip is in a range of 400–600°C. Obviously, the fire spread will not occur if the flame tip does not reach this position, that is, the flame does not exist above the object. In other words, the fire spread only occurs if the flame exists above the object.

From Table 4, it is clearly shown that in the tests with longitudinal flow in the vicinity of the fire and wood cribs, the second wood crib caught fire in about 1 min and 47 s, on average, and the third wood crib in about 2 min and 38 s. This implies that, at full scale, a vehicle 15 m behind a burning HGV will catch fire in about 8.5 min, and a third vehicle a further 15 m behind the second vehicle in only about

3 min more. The main reason for the rapid fire development in these model scale tests is due to the fire development of the first wood crib. In most of the tests, the first wood crib takes about 3 min to reach its peak heat release rate. Before this, the heat release rate increases almost linearly. At about 1 min and 47 s after ignition, the flame tip reaches above the second wood crib, and consequently ignites it. Although the second wood crib is not the main reason responsible for the fire spread to the third wood crib, it may be mainly responsible for a possible fourth wood crib. In addition, the second wood crib may also be responsible for the fire spread of the third wood crib if the peak HHR of the first wood crib is not large enough, that is, the flame length cannot extend to above the position of the third wood crib. It should, however, be pointed out that these numbers can only be used as an indication of the phenomena rather than actual values for a real scale scenario, as radiation and ignition processes do not scale well in the model tests.

Note that ignition time of the second wood crib in Test 4 was delayed, compared with that in Tests 7 and 8, and in former Tests 3 and 4 with longitudinal ventilation [7]. There are two reasons for this delay. Firstly, the ventilation velocity in Test 4 (present study) is 0.32 m/s, which is relatively lower than others, about 0.6 m/s. The lower ventilation velocity makes the growth rate also lower. This means that in Test 4 it takes much more time to reach a gas temperature as high as other tests. In addition, note that the second wood crib was placed beside the Nr 2 vent. In Test 4, the opened extraction vent (Nr2) removes the flame and smoke directly, which reduces the temperature beside the second wood crib, consequently, the wood crib ignites only when the fire grows sufficiently large. This partly proves that the extraction system can suppress fire development, that is, delay the ignition time of a secondary vehicle in the tunnel.

In an extraction system, the incoming air flow from both sides moves towards the fire source, which means that it is difficult for the fire to spread beyond the extraction vent. This is the main reason for the ability of the system to control the fire and smoke flow between the fire source and extraction vent in a single-point extraction system, or between two extraction vents in a two-point extraction system. Comparing data from Tests 4 and 11 indicates that the two-point extraction ventilation system seems to be more effective in suppressing the fire spread than the single extraction system, although the flame lies between the two extraction vents and the zone within which tenability criteria are not fulfilled gets larger. However, it should be pointed out that the fire and smoke can be controlled by both systems if appropriate ventilation systems are designed. Further, the fire spread in a single extraction system, that is, Test 4, may not occur if the second wood crib (vehicle) lies further away from the extraction vent.

Single-point extraction system

In a single-point extraction system, as shown in Figure 11, the exhaust volumetric flow rate through the extraction vent is a very important parameter. However, the exhaust volumetric flow rate varies significantly with the gas temperature of the

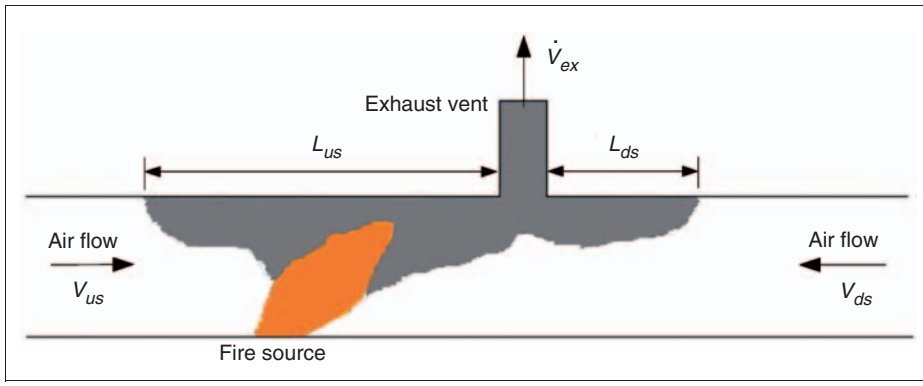

Figure 11. Schematic diagram of single-point extraction system.

smoke flow. This implies that different exhaust volumetric flow rates will be present at different locations of the pipe relative to the extraction vent, especially for a large fire which produces smoke flow with a very high gas temperature. Therefore, it is more reasonable to use the exhaust mass flow rate as a characteristic parameter of the extraction vent, rather than the exhaust volumetric flow rate. According to the law of mass conservation, the exhaust mass flow rate can be determined if the ventilation velocities on both sides are known. Here the focus is on the longitudinal ventilation velocities required to prevent the smoke flow on both sides, and not on the exhaust mass flow rate or the exhaust volumetric flow rate.

The principle of an effective single-point extraction system is expected to be that sufficient fresh air flows are supplied from both sides to constrain the fire and smoke in the zone between the fire source and the extraction vent point. The minimum ventilation velocity for each side is defined as the critical longitudinal ventilation velocity upstream of the fire source and downstream of the extraction vent, respectively. If the ventilation velocity is smaller than the critical velocity, the phenomenon of back-layering occurs. The distance between the extraction vent and the smoke front on the left-hand side is defined as the back-layering length upstream of the fire source, L_{us}, and the distance between the extraction vent and the smoke front on the right-hand side is defined as the back-layering length downstream of the extraction vent, L_{ds}, as shown in Figure 11.

The ventilation velocity upstream the fire source, V_{us}, should normally not be smaller than the critical velocity in a longitudinally ventilated tunnel, due to the fact that there is a little difference between this system and the longitudinal ventilation system upstream of the fire source (on the left-hand side). However, the phenomenon of control of smoke flow downstream of the fire source (on the right-hand side) is quite different.

Eight tests were conducted with a single-point extraction system. The heat release rate in these tests was in a range of 52.6–190.6 kW, corresponding to 133–484 MW at full scale. The volumetric flow rate is strongly dependent on the temperature. The mass flow rate for the extraction vent, which is a more reasonable

Table 5. The back-layering lengths upstream of the fire and downstream of the extraction vent.

	HRR	Upstream		Downstream		Extraction vent	
Test no.	Q_{max} (kW)	V_{us} (m/s)	L_{us} (m)	V_{ds} (m/s)	L_{ds} (m)	$\dot{V}_{ex}$ (m^3/s)	$\dot{m}_{ex}$ (kg/s)
1	97.7	0.61	<0.38	1.01	<0.5	0.15	0.16
2	65.1	0.25	1.63–2.87	1.27	0*	0.14	0.15
3	52.6	0.26	2.1–3.35	0.73	<0.53	0.09	0.10
4	86.6	0.32	1.63–2.87	1.18	<1.1	0.14	0.15
5	57.6	0.34	1.0–2.1	0.25	0.53–1.77	0.056	0.06
6	83.9	0.59	<0.38	0.90	<1.1	0.14	0.16
7	158.3	0.57	<0.38	1.05	<0.5	0.14	0.17
8	190.6	0.58	<0.38	0.94	<0.5	0.14	0.15

*No back-layering observed during the test.

parameter to use for an extraction system, is in a range of 0.06–0.16 kg/s. This corresponds to 152–406 kg/s at full scale, that is, a volumetric flow rate of 127–338 m^3/s for fresh air. Based on the experiments carried out in Lacroix et al., [20] the geometry of the extraction vents has little effect on the performance of the extraction ventilation system. The effect of the geometry of an extraction vent is therefore not discussed here.

Analysis of the gas temperature distribution below the ceiling determines whether the fire and smoke flow was controlled or not and the range in which back-layering disappears. The data concerning back-layering length upstream of the fire source and downstream of the extraction vent are given in Table 5.

Firstly, it is considered whether there is a critical total mass flow rate or total volumetric flow rate in an extraction vent for control of fire and smoke in an acceptable zone, and secondly whether a critical total flow rate is needed, regardless of the longitudinal ventilation velocities on both sides. From Table 5, it is clearly shown that Test 5, with an exhaust mass flow rate of 0.06 kg/s, is the worst case. Test 2, 3, and 4 are not optimal either, although the total mass flow rate in the exhaust pipe is up to 0.1 kg/s or even 0.15 kg/s. The reason is that the longitudinal ventilation velocities upstream of the fire source in Tests 2 and 4 are too low, less than 0.4 m/s. The reason for this is that the longitudinal ventilation velocities on both sides are dependent on the ventilation system of the whole tunnel, and the longitudinal velocity on the one side may be very low even though the total flow rate is large. This phenomenon is usually related to different lengths of the tunnel tube and thereby a different flow resistance on each side of the exhaust opening. Consequently, the total volumetric flow rate in an extraction vent cannot be controlled independent of the ventilation velocities on both sides. Incoming air flows, with a high enough ventilation velocity on both sides, should be created to control the smoke from flowing upstream of the fire source and downstream of the extraction vent.

From Table 5, it is shown that in Tests 2–5, the longitudinal ventilation velocities upstream of the fire source were about 0.3 m/s, which is about half the critical velocity in a longitudinally ventilated tunnel, and the back-layering lengths are in a range of 5 H–15 H, corresponding to a range of 20–70 m at full scale. In Tests 1, 6, 7, and 8, with longitudinal ventilation velocities of about 0.6 m/s upstream of the fire source and of 0.90—1.05 m/s downstream of the extraction vent, the fire and smoke flow can be considered as being completely controlled on both sides. The corresponding exhaust mass flow rate is about 0.15 kg/s, corresponding to 317 kg/s at full scale and maximum heat release rate in these tests is up to 190.6 kW, corresponding to 484 MW at full scale.

Upstream of the fire source. It is proposed that the phenomenon of back-layering upstream of the fire source is the same as the back-layering phenomenon for the longitudinal ventilation system. In the following, this hypothesis is discussed and evaluated.

Figure 12 shows the back-layering length as a function of the longitudinal ventilation velocity upstream of the fire source for the single-point extraction ventilation. In this figure, 'smoke' means that back-layering was observed and 'no smoke' implies no observed smoke at this position, for a given longitudinal ventilation velocity. Consequently, the actual back-layering length should lie between data point for 'smoke' and data point for 'no smoke'. The data for different heat release rates can be correlated into a single form, as shown in Figure 12. The reason for this is that for a very large fire, the back-layering length upstream of the fire source

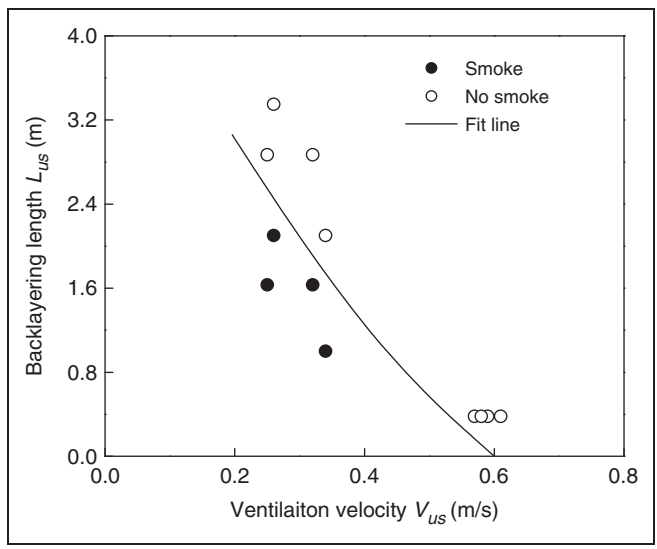

Figure 12. Back-layering length and ventilation velocity upstream of the fire in tests with single-point extraction ventilation.

is independent of the heat release rate, that is, the dimensionless heat release rate is over 0.15 [21]. For a very large fire, the combustion near the fire source is confined due to the tunnel geometry and the temperature of smoke flow is almost constant. This means that the critical velocity is only a weak function of the fire heat release rate. It is shown in Figure 12 that the back-layering length decreases with the ventilation velocity, and the critical velocity can be considered as about 0.6 m/s for this model tunnel. This value corresponds to 2.9 m/s at full scale.

Further, a comparison of data from point extraction ventilation tests with longitudinal ventilation tests [7] was made. For the comparison, the dimensionless ventilation velocity and dimensionless back-layering length from Li et al. [21] are used here, due to differences in the geometry of these model tunnels. These two terms are respectively defined as:

$$L^*_{us} = \frac{L_{us}}{H} \tag{14}$$

and:

$$V^*_{us} = \frac{V_{us}}{\sqrt{gH}} \tag{15}$$

Figure 13 shows the comparison of data from these two series of tests. All the data for the dimensionless back-layering length upstream of the fire are plotted as a function of the dimensionless ventilation velocity. An observed back-layering length of zero implies that there is no back-layering in this test.

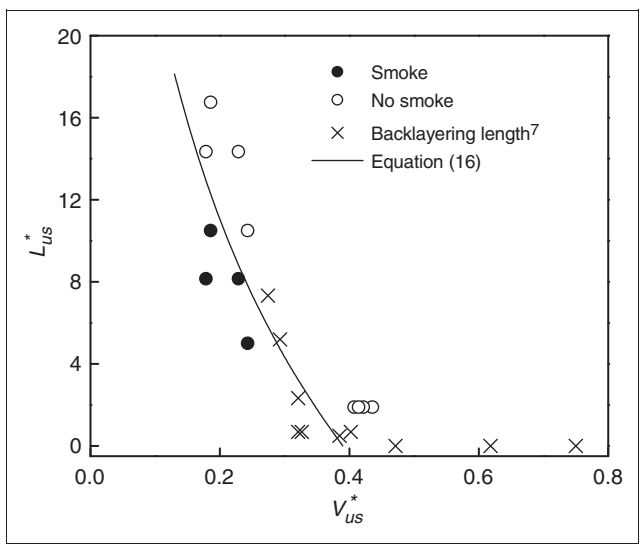

Figure 13. Comparison of data from point extraction tests with longitudinal ventilation tests.

It is clearly shown in Figure 13 that data from these two tests can be correlated reasonably well with the proposed line. This confirms that there is little difference between this system and the longitudinal ventilation system upstream of the fire source (on the left-hand side). The proposed line can be expressed as:

$$L^*_{us} = 16.5 \ln\left(0.39/V^*_{us}\right) \tag{16}$$

According to Equation (16), the critical velocity can be easily determined by forcing the dimensionless back-layering length to be zero. Equation (16) has a form similar to the correlation proposed in Li et al. [21] but with somewhat smaller coefficients. The dimensionless critical velocity is 0.39 in Equation (16) and 0.43 for the correlations in Li et al. [21]. The reason for the slightly lower value here could be that for the experiments in Li et al., [21] the fire source was set at floor level, which was not the case in these series of model scale tests.

In a single-point extraction system, in order to control the smoke flow between the fire source and the point extraction vent, smoke back-layering has to be prevented. It is now known how to prevent any smoke flow upstream of fire source. Alternatively, it may be better to just confine the smoke flow to an acceptable zone, which reduces the required capacity of the exhaust fans and preserves smoke stratification. This means that only a longitudinal flow with a ventilation velocity smaller than the critical velocity, called confinement velocity, is required to be created in the tunnel to suppress the back-layering upstream of the fire source. From Figure 13, it is shown that the ventilation velocity can be reduced to 50% of the critical velocity upstream of the fire source if a back-layering length of about 12 times the tunnel height is permitted, and 75% of critical velocity if a back-layering length of about 5 times the tunnel height is permitted.

Downstream of the extraction vent. From Table 5, it is shown that most of experimental data indicate that the back-layering lengths downstream of the extraction vent are <0.5 m. This suggests the smoke flow downstream of the fire source was controlled completely or confined to an acceptable zone in the tests. The corresponding ventilation velocity downstream of the fire source lies mainly in a range of 0.73–1.27 m/s.

It also seems that the back-layering length downstream of the fire source is independent of the heat release rate for a very large fire in a tunnel. The back-layering lengths are plotted as a function of the ventilation velocity downstream of the extraction vent, as shown in Figure 14. If the back-layering length is <0.5 m, the smoke flow can be regarded roughly as being completely controlled. From Figure 14, it is shown that the critical velocity for smoke control downstream of the extraction vent when back-layering disappears is in a range of 0.7–1.0 m/s. A value of 0.8 m/s should be sufficient to prevent the smoke flow downstream of the extraction vent. Note that this value is about 1.3 times the critical velocity in a longitudinally ventilated tunnel.

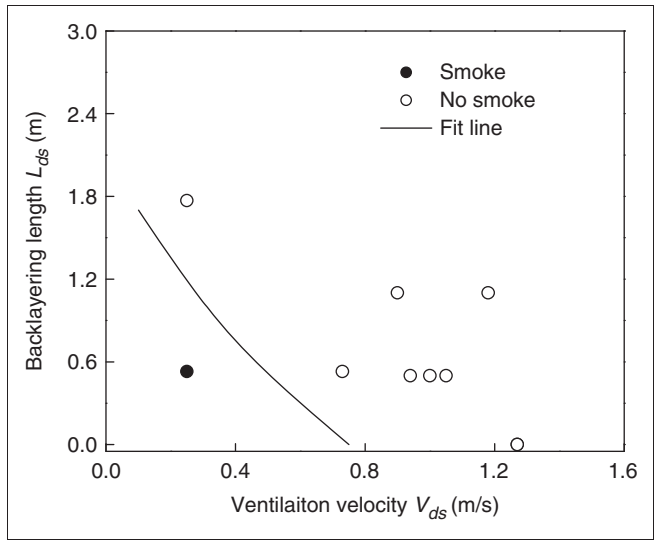

Figure 14. Back-layering length and ventilation velocity downstream of the fire source in model scale tests with single-point extraction ventilation.

Based on the above analysis, it can be concluded that in a single-point extraction system, fire and smoke flows upstream and downstream of the fire source can be fully controlled if the ventilation velocity upstream of the fire source is up to 0.6 m/s (2.9 m/s at full scale), and downstream of the extraction vent about 0.8 m/s (3.8 m/s at full scale), for a HGV fire or even several HGVs with heat release rate up to 484 MW. The effects of the configuration and location of the HGVs on such requirements has not been investigated. Under these conditions, the mass flow rate through the extraction vent is about 0.134 kg/s, corresponding to 340 kg/s at full scale, that is, a volumetric flow rate of 284 m^3/s for fresh air. This indicates that there is a critical mass flow rate of the extraction vent or a critical total volumetric flow rate of the incoming air flows from both sides. However, the ventilation velocities on both sides above all should fulfill the requirements for control of fire and smoke flow between the fire source and the extraction vent. Note that the critical velocity required to prevent smoke back flow upstream of the fire source is almost equal to the critical velocity in a longitudinally ventilated tunnel, and the critical velocity downstream of the extraction vent can be regarded as 1.3 times the critical velocity in a longitudinally ventilated tunnel.

Further, smaller ventilation velocities on both sides can be used for just confining the fire and smoke flow in acceptable zones. This can efficiently reduce the capacity of the extraction vent and the geometry of the extraction vent. However, the ventilation velocity cannot be too small, that is, not be smaller than 0.75 times the critical velocity to prevent the fire and smoke flow upstream of the fire source

from spreading to a distance of about 5 times the tunnel height. This also works for smoke control downstream of the extraction vent, as shown in Figure 14.

Data from tests with different vent geometries show that the fire and smoke flow in tests with a vent geometry of 0.26 m × 0.1 m can also be controlled or confined to an acceptable zone for a single-point extraction system. However, the vent geometry of 0.26 m × 0.2 m is recommended, corresponding to 6 m × 4.6 m at full scale, since it is easier to keep the ventilation velocity through the vent at a low level.

Two-point extraction system

Figure 15 gives a schematic diagram of a two-point extraction system. It is designed to be capable of producing a dual inward flow to control the fire and smoke flow. The ventilation velocity across the fire source is dependent on the ventilation system of the specific tunnel. In most cases the systems are not symmetrical, and there is always a longitudinal flow across the fire source. In that case the fire source leans toward one side, as shown in Figure 15. If the ventilation velocity across the fire source is very small, the smoke stratification will be preserved well in the zone between the two extraction vents. Of course, the gas temperature in this zone is very high. However, the dangerous region can be confined by reducing the interval between two extraction vents, and the environment in the vicinity of the fire is not the focal point. Here, how to control the fire and smoke flow on both sides is the focus. Three model scale tests with this system were carried out.

For a two-point extraction system, as shown in Figure 15, the back-layering length on the left-hand side is defined as the distance between the smoke front and the left extraction vent. In a similar way the definition of the back-layering length on the right-hand side can be made.

According to the gas temperature distribution, the back-layering lengths on both sides of the tunnel can be given, as shown in Table 6. During these tests, only the total mass flow rate and total volumetric flow rate of the extraction vents are measured.

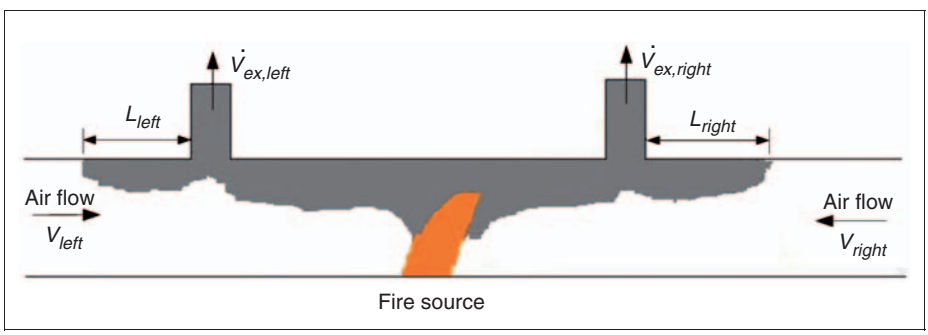

Figure 15. Schematic diagram of a two-point extraction system.

Table 6. Back-layering length on both sides of the tunnel in tests with two-point extraction system.

Test no.	HRR Q_{max} (kW)	Left V_{left} (m/s)	Right L_{left} (m)	Right V_{right} (m/s)	Right L_{right} (m)	Extraction vent $\dot{V}_{ex,tot}$ (m^3/s)	Extraction vent $\dot{m}_{ex,tot}$ (kg/s)
9	51.4	0.40	0.53–1.77	0.79	<1.1	0.09	0.11
10	52.6	0.52	<0.53	0.99	<1.1	0.14	0.16
11	57.6	0.36	0.53–1.77	0.81	<1.1	0.09	0.10

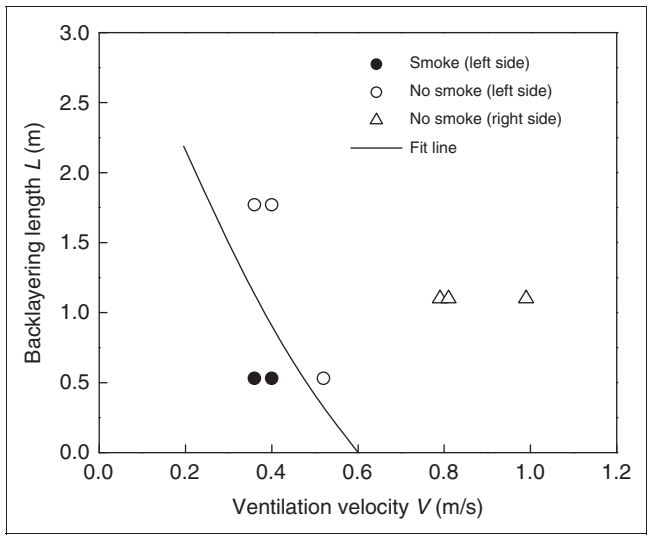

Figure 16. Back-layering length and ventilation velocity in model scale tests with two-point extraction ventilation system.

The low values of ventilation velocity of the air flow near the fire site (between the fire source and the exhaust vents) are difficult to measure. However, according to observations during these tests, the fire plume nearly did not lean toward any side, which suggests that the fires were nearly symmetrical. This means that the ventilation flow should also be symmetrical. The scenario is similar to a fire in a tunnel with natural ventilation or an enclosure with large windows and roof extraction vents. The fresh air is introduced from both portals by the extraction system and by the fire, and it flows towards the fire in the lower layer. A characteristic of this system is the lower heat release rate due to the absence of forced ventilation. It can be seen from Table 6 that the heat release rates are close to each other, that is, about 54 kW, corresponding to 137 MW at full scale, in these tests with a two-point extraction system.

Due to the symmetry of the scenario in these tests, data for both sides can be plotted in a single form. Figure 16 shows the back-layering length as a function of the ventilation velocity in the model scale tests with two-point extraction ventilation. It can be concluded that the ventilation velocity on each side of the vents should be greater than about 0.6 m/s, corresponding to 2.9 m/s at full scale, to completely confine the fire and smoke flow in the zone between two extraction vents. Note that this value is almost equal to the critical velocity in a longitudinally ventilated tunnel. Of course, it is more reasonable to simply confine the fire and smoke to an acceptable zone, that is, to permit back-layering to some extent. It is also shown that a value of 0.52 m/s, corresponding to 2.5 m/s at full scale, can prevent the fire and smoke flow from spreading to a distance of 3 times the tunnel height.

If the same intervals between the extraction vents are used in a tunnel, obviously, the smoke zone of a two-point extraction system will inherently be wider than that with a single-point extraction system. Therefore the extraction vents for a single-point extraction system can be arranged with larger intervals.

Conclusion

Model scale experiments show that extraction vents at the ceiling level of a tunnel provide very effective smoke control for a large fire. The extraction vent flows and the inward air flows that are thereby produced in the tunnel will constrain the flame and smoke within the zone between the extraction vent and the fire source in a single extraction system, or between the two opened extraction vents in a two-point extraction system. This suggests that smoke flow from even a very large fire in a tunnel, that is, a HGV fire, can be controlled by an appropriate extraction ventilation system.

An effective extraction system has been shown to be established when sufficient fresh air flows are supplied from both sides to confine the fire and smoke to the zone between the fire source and the extraction vent for a single-point extraction ventilation system, or between two extraction vents for a two-point extraction ventilation system. The fire and smoke flow could not be confined if only the flow rate in the extraction vents were controlled, regardless of the ventilation velocities on both sides. In a single extraction system, fire and smoke flows upstream and downstream of the fire source can be fully controlled, if the ventilation velocity upstream of the fire source is greater than about 0.6 m/s (2.9 m/s at full scale), and the ventilation downstream of the extraction vent is above about 0.8 m/s (3.8 m/s at full scale), for a HGV fire or even several HGVs with heat release rate up to about 500 MW. These are considerably lower values than obtained by Vauquelin et al. [5,6] using a cold gas mixture. Under these conditions, the mass flow rate through the extraction vent is about 0.134 kg/s, corresponding to 340 kg/s at full scale, that is, a volumetric flow rate of 284 m^3/s for fresh air. In a two-point extraction system, the longitudinal ventilation velocity on the each side should be greater than about 0.6 m/s, corresponding to 2.9 m/s at full scale, to

completely confine the fire and smoke flow in the zone between the two extraction vents.

The extraction system will also significantly reduce the risk of the fire spreading outside the fire and smoke zone, as a result of removing the flame and heat produced by the fire from the tunnel. However, in the near proximity of the fire site, the fire spread cannot be prevented. Fire spread to a neighboring wood crib occurs when the gas temperature below the ceiling and above the wood crib rises to about 600°C. Experimental data suggest that in a real tunnel, a vehicle 15 m behind a (simulated) burning HGV would catch fire in about 9 min, and a third vehicle 15 m further behind the second vehicle would catch fire in about 3 more min, mainly due to heat from the first vehicle. The experiments clearly show the 'snowball' effect resulting from HGVs close to each other. The fire spread rate is in quite good agreement with the Runehamar tunnel trials, where 'targets' were placed 15 m from the fire in order to simulate the effects of possible spread of the fire.

The heat release rate, fire growth rate, maximum excess gas temperature beneath the ceiling, and heat flux were also investigated. A stoichiometric line fits the experimental data of the fuel mass loss rate per unit fuel surface area well when the ventilation velocity is less than 0.35 m/s. For a higher ventilation velocity, the fuel mass loss rate per unit fuel surface area is not sensitive to the ventilation velocity. This means there is an upper limit of about 0.013 kg/(m^{2}s) for the wood cribs used here, which correlates well with the ideal value found in [17] based on the assumption that all heat losses were reduced to zero. The fire growth rate increases linearly with the ventilation velocity. The fire growth rate is nearly 3 times larger than that in free burn tests, when the longitudinal ventilation velocity equals 1 m/s, corresponding to 4.8 m/s at full scale. The dimensionless maximum excess temperature lies mainly in a range of 3.1–3.75, corresponding to a maximum excess temperature of 900–1100°C. It seems that the maximum gas temperature beneath the tunnel ceiling is a weak function of the heat release rate and the ventilation velocity for a HGV fire with a heat release rate over 100 MW. The total heat flux can be correlated well using the gas temperature beneath the tunnel ceiling.

Nomenclature

A = cross-sectional area of the tunnel (m^2)
A_s = total fuel area (m^2)
c_p = heat capacity of air (kJ/kg·K)
E = total calorific value (kJ)
F = view factor
g = gravity acceleration (m/s^2)
H = tunnel height (m)
H_T = net heat of complete combustion (kJ/kg)
L = Length scale (m)
L_{us} = back-layering length upstream (m)
L_{ds} = back-layering length downstream (m)

L_{left} = back-layering length left side (m)
L_{right} = back-layering length right side (m)
L^*_{us} = dimensionless back-layering length upstream (m)
m = fuel mass (kg)
$\dot{m}_a$ = total air mass flow rate inside the tunnel (kg/s)
$\dot{m}_{ex,\,tot}$ = total mass flow rate of an exhaust vent (kg/s)
$\dot{m}_f$ = fuel mass loss rate (kg/s)
$\dot{m}_{f,\,\max}$ = maximum fuel mass loss rate during a test (kg/s)
$\dot{m}_{f,\,stoi}$ = stoichiometric fuel mass loss rate (kg/s)
q'' = total heat flux (kW/m^2)
$q''_{\max}$ = maximum heat release rate per unit fuel area (kW/m^2)
Q = total heat release rate (kW)
$Q_{\max}$ = maximum heat release rate during a test (kW)
T = gas temperature (K)
T_a = ambient temperature (K)
T_{cf} = ceiling temperature (K)
$\Delta T_{\max}$ = maximum excess gas temperature beneath the ceiling (K)
t = time (s)
V = gas velocity (m/s)
V_{us} = air velocity upstream (m)
V_{ds} = air velocity downstream (m)
V_{left} = air velocity left side (m)
V_{right} = air velocity right side (m)
V^*_{us} = dimensionless air velocity upstream (m)
$\dot{V}_{ex,\,tot}$ = total volume flow rate of a exhaust vent (m^3/s)
X_{O_2} = volume fractions of oxygen at the measuring station (dry)
X_{CO_2} = volume fractions of carbon dioxide at the measuring station (dry)
X_{0,O_2} = volume fraction of oxygen in the incoming air (ambient)
$X_{0,\,CO_2}$ = volume fraction of carbon dioxide measured in the incoming air (ambient)
X_f = distance from the centerline of the fire source (m)

Greek symbols

ρ_a = ambient density (kg/m^3)
σ = Stefan–Boltzmann constant (kW/m^2·K^4)
ε = Emissivity
χ = ratio of effective heat of combustion to net heat of complete combustion

Acknowledgments

This study was sponsored by the Swedish Fire Research Board (BRANDFORSK) and the SP Tunnel and Underground Safety Centre. We also want to acknowledge Dr Margaret McNamee and Dr Anders Lönnermark for their valuable comments.

References

1. Ingason H and Lönnermark A. Heat release rates from heavy goods vehicle trailers in tunnels. *Fire Safety Journal* 2005; Vol. 40: 646–668.

2. Lönnermark A and Ingason H. Gas temperatures in heavy goods vehicle fires in tunnels. *Fire Safety Journal* 2005; Vol. 40: 506–527.
3. Massachusetts Highway Department and US Federal Highway Administration. *Memorial tunnel fire ventilation test program*. Test Report, Boston, 1995.
4. Studiensgesellschaft Stahlanwendung e. V. *Fires in transport tunnels: Report on full-scale tests*. Eureka Project EU 499 FIRETUN, Düsseldorf, Germany, 1995.
5. Vauquelin O and Telle D. Definition and experimental evaluation of the smoke 'confinement velocity' in tunnel fires. *Fire Safety Journal* 2005; Vol. 40: 320–330.
6. Vauquelin O and Mégret O. Smoke extraction experiments in case of fire in a tunnel. *Fire Safety Journal* 2002; Vol. 37: 525–533.
7. Ingason H and Li YZ. Model scale tunnel fire tests with longitudinal ventilation. *Fire Safety Journal* 2010; Vol. 45(6–8): 371–384.
8. Heskestad G. Modeling of enclosure fires. In: *Proceedings of the Fourteenth Symposium (International) on Combustion*, Pittsburgh, USA, The Combustion Institute, 1973.
9. Heskestad G. Physical modeling of fire. *Journal of Fire & Flammability* 1975; Vol. 6: 253–273.
10. Quintiere JG. Scaling applications in fire research. *Fire Safety Journal* 1989; Vol. 15: 3–29.
11. Saito N, Yamada T, Sekizawa A, Yanai E, Watanabe Y and Miyazaki S. Experimental study on fire behavior in a wind tunnel with a reduced scale model. In: *Second International Conference on Safety in Road and Rail Tunnels*, Granada, Spain, 1995, pp. 303–310.
12. Janssens M and Parker WJ. Oxygen consumption calorimetry. In: Babrauskas V, Grayson TJ (eds) *Heat release in fires*. London: E & FN Spon, 1995, pp.31–59.
13. Ingason H. Fire dynamics in tunnels. In: Carvel RO, Beard A.N (eds) *The handbook of tunnel fire safety*. London: Thomas Telford Publishing, 2005, pp.231–266.
14. McCaffrey BJ and Heskestad G. Brief communications: a robust bidirectional low-velocity probe for flame and fire application. *Combustion and Flame* 1976; Vol. 26: 125–127.
15. Ingason H and Li YZ. *Model scale tunnel fire tests – point extraction ventilation*. SP Report 2010:03, National Testing and Research Institute, Borås, Sweden, 2010 (SP Swedish).
16. Croce PA and Xin Y. Scale modeling of quasi-steady wood crib fires in enclosures. *Fire Safety Journal* 2005; Vol. 40: 245–266.
17. Tewarson A and Pion RF. Flammability of plastics. I. Burning intensity. *Combustion and Flame* 1976; Vol. 26: 85–103.
18. McCaffrey BJ. *Purely buoyant diffusion fames: some experimental results*. NBSIR 79-1910. Gaithersburg, MD, USA: National Institute of Standards and Technology, 1979.
19. Kurioka H, Oka Y, Satoh H and Sugawa O. Fire properties in near field of square fire source with longitudinal ventilation in tunnels. *Fire Safety Journal* 2003; Vol. 38: 319–340.
20. Lacroix D, Chasse P and Muller T. Small scale study of smoke trap door system. In: *The 8th International Symposium on Aerodynamics and Ventilation of Vehicle Tunnels*, Liverpool, UK, BHR Group, 1994, pp.409–438.
21. Li YZ, Lei B and Ingason H. Study of critical velocity and backlayering length in longitudinally ventilated tunnel fires. *Fire Safety Journal* 2010; Vol. 45(6-8): 361–370.